

Electroformation of Coatings Modified with Silver on Magnesium Alloys for Biomedical Applications

A.P. Loperena^a, A.D. Forero López^a, L.I. Brugnoli^b,
I.L. Lehr^{a,*} and S.B. Saidman^a

^a Electrochemical Engineering and Corrosion Institute, Chemical Engineering Department, South National University, CONICET, Bahía Blanca, Argentina.

^b South Biological and Biomedical Research Institute, Biology, Biochemistry and Pharmacy Department, CONICET, Bahía Blanca, Argentina.

Received April 17, 2018, Accepted August 24, 2020

Abstract

Three different films modified with silver species were considered to enhance the corrosion resistance of AZ91D Mg alloy and to impart its surface with antibacterial activity. First, coatings were electrodeposited under potentiostatic conditions in electrolyte solutions containing Na₂MoO₄ and/or Ce(NO₃)₃ as main compounds, and H₂O₂, ascorbic acid or citric acid as additives. Incorporation of silver species was done by immersion of the samples in AgNO₃ solutions. The obtained modified films were characterized by scanning electron microscopy (SEM) and X-ray diffraction (XRD). The corrosion protection properties of the films were examined in a simulated physiological solution by open circuit measurements, linear polarization and electrochemical impedance spectroscopy (EIS). The antibacterial effect of the coatings was evaluated using *Escherichia coli* bacteria. Cerium and molybdenum-based coating modified with silver provides superior antibacterial and anticorrosive properties compared to the other films studied.

Keywords: AZ91D Mg alloy corrosion protection; cerium and molybdenum coatings; and silver modification.

Introduction

Magnesium and its alloys are biodegradable and biocompatible materials which constitute an advantage for developing temporary therapeutic devices [1, 2]. However, these materials present poor corrosion resistance under physiological conditions, which has delayed their introduction into therapeutic applications to date [2]. AZ91D is one of the most commonly used magnesium alloys and its

* Corresponding author. E-mail address: ilehr@uns.edu.ar

corrosion resistance depends on the presence of impurities acting as an active cathode in the microstructure [3].

In order to improve the corrosion resistance of Mg and its alloys in physiological solutions, several environmental friendly methods have been developed. Among them, treatments that modify the oxide surfaces are known for the low cost and simplicity of the operation. Anodization is one of the most popular surface protective treatments for these biodegradable materials. In contrast to other surface treatments, anodization can produce a relatively thick, hard, adherent and abrasion-resistance film [4].

It was shown that molybdenum acts as a localized corrosion inhibitor for stainless steel, when it is present in the electrolyte solution as Mo(VI) [5, 6]. The use of molybdate in different treatments to protect Mg alloys against corrosion has been the subject of various works [7-9]. Molybdate anions have many advantages, such as low toxicity and high stability in aqueous media [10, 11]. In a previous work, we showed that the anodization of the AZ91D magnesium alloy, in molybdate solutions, applying low potentials, allowed obtaining coatings with good anticorrosive performance [12]. The improvement in the corrosion resistance is associated with the presence of molybdenum species in the obtained film.

At the same time, cerium-based coatings on magnesium alloys have been intensively studied [13, 14]. Several works have reported that these coatings increase the corrosion resistance of magnesium biodegradable alloys in simulated physiological media. As magnesium alloy oxidizes, the reduction of hydrogen ions occurs. This hydrogen discharge promotes the reaction of OH⁻ with cerium ions to form insoluble Ce(OH)₃ and Ce(OH)₄, which are present in the film [15, 16]. Moreover, it is known that the use of H₂O₂ as additive in the generation solution allows the formation of more compact films [17-20]. The presence of hydrogen peroxide is associated with more protective cerium coatings, since it promotes the formation of Ce(IV) oxides [21-23]. Furthermore, it has been demonstrated that the cerium coating obtained by electrochemical techniques has better anticorrosive properties [24]. We have reported the formation of cerium-based coating prepared from a solution containing Ce(NO₃)₃, H₂O₂ and ascorbic acid (HAsc) on AZ91D alloy [25]. The synthesized film showed a superior corrosion performance in a simulated physiological solution, compared with those films formed in the absence of HAsc [25]. The improvement in the anticorrosive properties is associated with the combination of the characteristics of the cerium oxides and the inhibitor effect of the additive.

More recently, we have investigated the generation of a coating on AZ91D Mg alloy in a solution containing Ce(NO₃)₃, Na₂MoO₄ and C₆H₈O₇ (H₃Cit) [26]. Preliminary results have shown superior corrosion efficiency compared to the coatings mentioned before. The obtained film is uniform and it is mainly composed by CeO₂, Ce₂O₃, MoO₃, MoO₂, MgO and Mg(OH)₂.

On the other hand, surfaces of metallic devices are susceptible to colonization, proliferation and biofilm formation by pathogenic bacteria. In this context, antibacterial surface treatments appear as a way of limiting bacteria transfer. Silver species are recognized as excellent antimicrobial agents, because they

have a strong toxicity towards a wide range of microorganisms. Thus, the incorporation of silver species on biomaterials surfaces is receiving increasing attention for possible uses in medical devices [27-29]. Silver modified coatings have shown to confer antibacterial and corrosion protection properties to magnesium based substrates for biomedical applications [29-30]. Moreover, Liu et. al. demonstrated that pure Mg alloyed with metallic silver presents antibacterial properties [31].

The main objective of the present work was to study the incorporation of silver species into different coatings obtained by us, which were previously mentioned in this section. Optimal experimental conditions were determined in order to obtain coatings with *simultaneous antibacterial* and anticorrosive properties in a simulated physiological solution. The influence of the concentration of the AgNO₃ solution was analysed on the anticorrosive performance.

Experimental procedures

Materials and methods

The working electrodes were prepared from rods of die-cast AZ91D magnesium alloy (composition: 8.978% Al, 0.6172% Zn, 0.2373% Mn, 0.2987% Si, 0.1189% Cu, 0.00256% Ni, 0.0176% Fe, 0.00164% Ca, 0.01154% Zr and the remainder was Mg). The rods were embedded in a Teflon holder with an exposed area of 0.070 cm².

Before each experiment, the exposed surfaces were polished to a 1000 grit finish using SiC, then degreased with acetone and washed with triply distilled water. Following this pretreatment, the electrode was immediately transferred to the electrochemical cell. All potentials were measured against saturated Ag/AgCl and a platinum sheet was used as counter electrode. The cell was a 20 cm³ Metrohm measuring cell.

Electroformation of the films was performed on AZ91D Mg alloy as follows:

- Molybdenum-based coatings (Mo-coat).

The film was obtained at 1.0 V, during 2700 s, in a solution containing 0.25 M of dehydrated sodium molybdate (Na₂MoO₄·2H₂O) [12].

- Cerium-based coating (Ce-coat).

The film was obtained at - 0.75 V, during 1800 s, in a solution containing 50 mM of Ce(NO₃)₃, 6 mM of H₂O₂ and 5 mM of HAsc [25].

- Cerium and Molybdenum-based coatings (Ce-Mo-coat).

The film was formed at - 0.30 V, during 1800 s, in a solution containing 30 mM of Ce(NO₃)₃, 15 mM of Na₂MoO₄ and 10 mM of H₃Cit [26].

Electrochemical measurements were done using an Autolab PGSTAT 128N potentiostat-galvanostat and a VoltaLab40 PGZ301 Potentiostat. The frequency used for the impedance measurements was changed from 100 kHz to 10 mHz, and the signal amplitude was 10 mV. The used scanning microscope was a SEM Carl Zeis EVO 40 HV. X-ray diffraction analysis was carried out using a Rigaku

X-ray diffractometer (model Dmax III-C) with Cu K α radiation and a graphite monochromator.

The corrosion behavior was evaluated in a Ringer solution at 37 °C by the variation of the open circuit potential (OCP) as a function of time, by potentiodynamic method and by electrochemical impedance spectroscopy (EIS). The electrodes were allowed to equilibrate at a fixed voltage before the ac measurements. The composition of the Ringer solution is (per 1 L) 8.60 g of NaCl, 0.30 g of KCl and 0.32 g of CaCl $_2$ ·2H $_2$ O.

The Tafel tests were carried out by polarization from cathodic to anodic potentials with respect to the open circuit potential at 0.001 Vs $^{-1}$ in a Ringer solution. Estimation of corrosion parameters was realized by the Tafel extrapolation method. The extrapolation of anodic and cathodic lines for charge transfer controlled reactions gave the corrosion current density (i_{corr}) at the corrosion potential (E_{corr}). All experiments were conducted approximately 30 min after immersion in the Ringer solution. Each set of experiments was repeated two to four times to ensure reproducibility.

Film adhesion was tested measuring the necessary force to peel-off the film using a Scotch® Magic™ double coated Tape 810 (3M) and a Mecmesin basic force gauge (BFG 50N).

The antibacterial activity against the Gram-negative bacteria *Escherichia coli* was evaluated by a modified Kirby-Bauer technique [33]. The method was previously standardized by adjusting the microbial inoculation rate and the volume of the agar medium layer. A stock culture of ATCC 25922 *E. coli* (stored at -70 °C in Trypticase Soy Broth (TSB) (BK 046HA, Biokar Diagnostics) supplemented with 20 % v/v glycerol (Biopack, Argentina) was used. A loop of frozen cells was cultured in TSB during 24 h at 37 °C, harvested by centrifugation at 5,000 x g for 10 min (Labofuge 200, Kendro, Germany), washed twice with phosphate-buffered saline (PBS: 0.15 mol l $^{-1}$ of NaCl, 0.05 mol l $^{-1}$ of KH $_2$ PO $_4$, 0.05 mol l $^{-1}$ of K $_2$ HPO $_4$, with pH 7.2) and then, cell pellets were suspended in PBS to achieve a population of ca. 7.0 log CFU (colony forming units) ml $^{-1}$ using a spectrophotometer (Thermo Spectronic Genesys 20, Thermo Electron Corporation, MA, USA). One milliliter of this suspension was mixed with twenty-five milliliters of Muller-Hinton Agar (BK, Biokar Diagnostics) melted and cooled at 43 °C, and then, placed on a Petridish. The coated electrodes were pressed onto bacteria-overlaid agar and were incubated at 37 °C for 48 h. Three replicates were made and the data were expressed as a growth inhibitory zone diameter (mm).

Results and discussion

Silver deposition

The three coatings, Mo-coat, Ce-coat and Ce-Mo-coat formed on the AZ91D Mg alloy were immersed in AgNO $_3$ solutions under open circuit potentials during 30 min. The influence of AgNO $_3$ concentration (0.025-0.075 M) on the coating formation was evaluated. Thus, the best conditions for obtaining the modified coatings were the following:

- Silver species on Mo-coat (Mo-coat/Ag)

A uniform *greyish coating* was formed on Mo-coat electrodes after immersion in 0.075 M AgNO₃ during 30 min. Lower concentrations of AgNO₃ generate localized Ag deposits. As shown in Fig. 1, silver dendrites were obtained in a large quantity on Mo-coat.

- Silver species on Ce-coat (Ce-coat/Ag)

A black film was obtained when Ce-coat was immersed in 0.025 M of AgNO₃ during 30 minutes. Coating delamination was observed for higher AgNO₃ concentrations. Fig. 2 shows the SEM micrograph of Ce-coat/Ag. The surface is partially covered with silver dendrites.

- Silver species on Ce-Mo-coat (Ce-Mo-coat/Ag)

An adherent *black coating* was formed on Ce/Mo-coat samples after immersion in 0.050 M AgNO₃ during 30 minutes. For this AgNO₃ concentration, the highest amount of silver dendrites was obtained (Fig. 3).

Several works reported three dimensional dendritic deposits of silver [34-35]. SEM images show that the Ce-Mo-coat/Ag presents few cracks, less pores and a denser structure, in comparison with Ce-coat/Ag and Mo-coat/Ag. XRD analysis of the coatings confirms the presence of silver in all the modified films (Fig. 4).

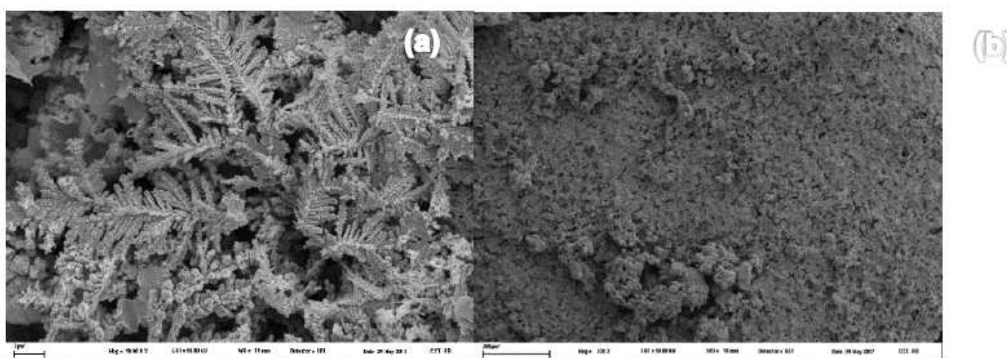


Figure 1. SEM images of silver dendrites electrodeposited on Mo-coat: (a) 200x and (b) 10000× magnification.

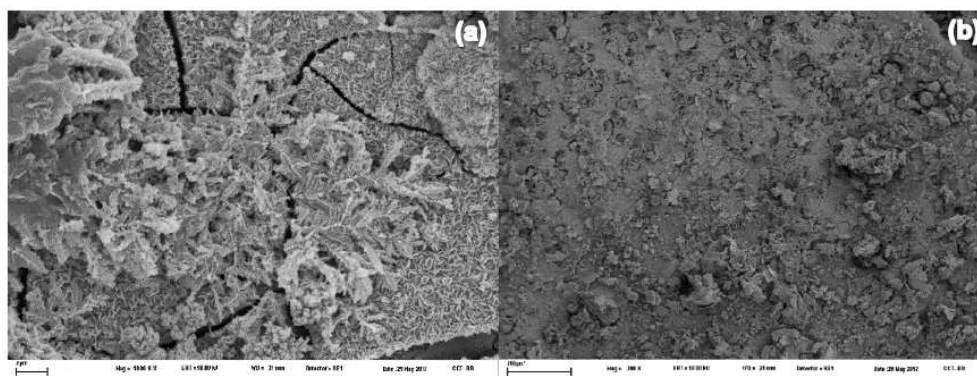


Figure 2. SEM images of silver dendrites electrodeposited on Ce-coat, (a) 200x and (b) 10000× magnification.

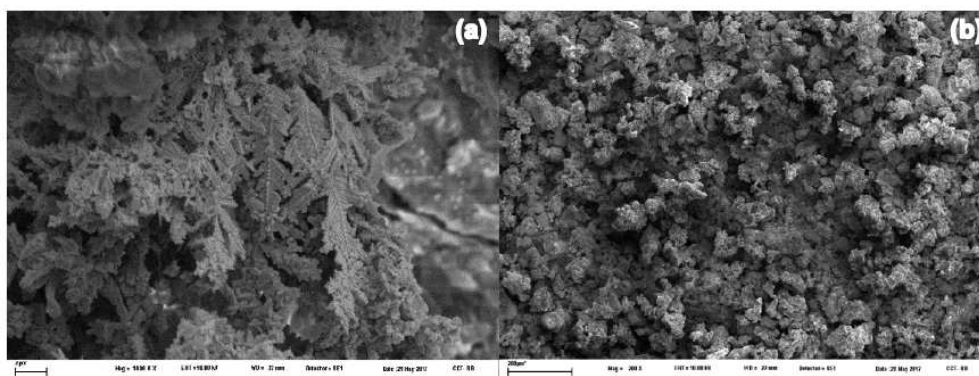


Figure 3. SEM images of silver dendrites electrodeposited on Ce-Mo-coat, (a) 200x and (b) 10000 \times magnification.

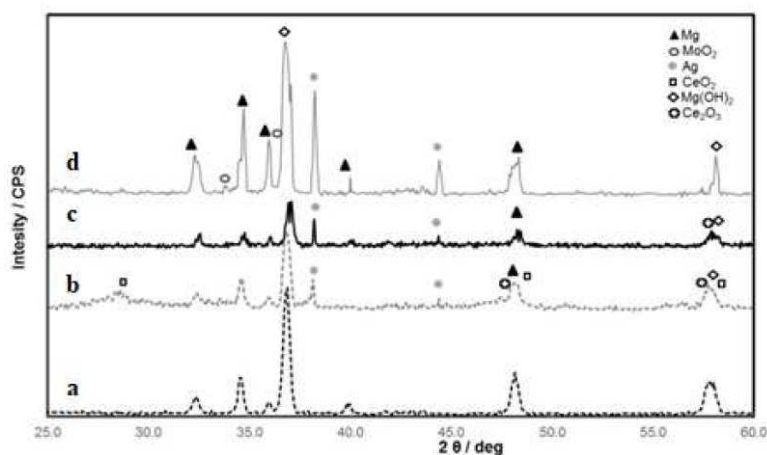


Figure 4. X-ray diffraction pattern of (a) bare AZ91D magnesium alloy, and the alloy covered with: (b) Ce-coat/Ag, (c) Mo-coat/Ag and (d) Ce-Mo-coat/Ag.

Antibacterial activity of silver-modified coatings

The antibacterial activity of modified films against the Gram negative bacteria *E. coli* ATCC 25922 was evaluated by determining the width of the inhibition zone around the coated surfaces. Unmodified films do not inhibit the growth of the bacteria, but an inhibition zone was observed in the case of Ag-modified coatings. The results were expressed as the growth inhibitory zone diameter (mm) for three replicates (Table 1). It can be seen that the Ce-Mo-coat/Ag exhibited a *better antibacterial performance* than the other modified films. Moreover, the modified films showed higher antibacterial activity when compared to other coatings formed on Mg substrates [30].

Table 1. Inhibition halo diameters of Mo-coat/Ag, Ce-coat/Ag and Ce-Mo-coat/Ag against ATCC 25922 *E. Coli* Gram negative bacteria. Unmodified coatings (Mo-coat, Ce-coat and Ce-Mo-coat) and the bare alloy do not present an inhibition halo.

Sample	Inhibition halo (mm)		
Mo-coat/Ag	6	7	6
Ce-coat/Ag	7	8	9
Ce-Mo-coat/Ag	10	12	14
Unmodified samples	----	----	----
AZ91D Mg alloy	----	----	----

The presence of inhibition zones indicates the release of silver to the surrounding environment and a subsequent antimicrobial effect. The antibacterial activity of silver modified coatings could be explained by the penetration of the released Ag^+ ions and colloid silver particles through the bacteria cell wall. Their complexation with enzymes in the cell membrane results in the inhibition of the enzymatic activity and in the bacteria death [36].

Adhesion measurements of silver-modified coatings

Table 2 shows the necessary force to peel-off the films. In all cases, only *mechanical polishing* removes the coatings. Ce-Mo-coat/Ag exhibits a higher adherence force than the other modified coatings.

Table 2. Adherence force obtained for the different coatings after peel-off testing.

Sample	Adherence force (N)
Mo-coat/Ag	11.45
Ce-coat/Ag	9.42
Ce-Mo-coat/Ag	49.53

Anticorrosion properties of silver-modified coatings

The polarization curves obtained in the Ringer solution for silver-modified coatings and for the uncoated substrate are presented in Fig. 5. A considerable *potential shift to more positive values is observed in the curves obtained for silver modified coatings*, indicating that all of them retard the active dissolution process of the bare alloy, which starts at -1.50 V ($\text{Ag}/\text{AgCl}_{\text{sat}}$). By comparing the curves, it is evident that the Ce-Mo-coat/Ag coating provides a significant improvement in the corrosion resistance of the substrate.

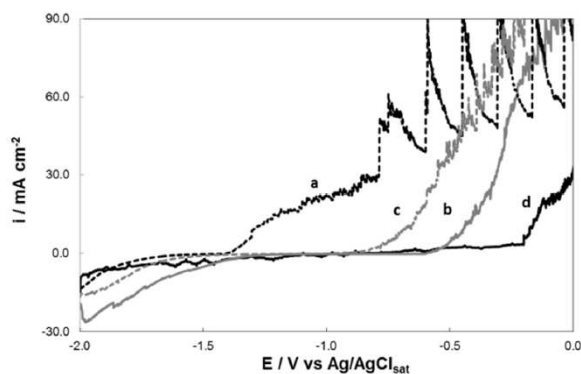


Figure 5. The polarization behavior in Ringer at 0.001 Vs^{-1} of: (a) bare AZ91D magnesium alloy, and the alloy covered with (b) Mo-coat/Ag, (c) Ce-coat/Ag and (d) Ce-Mo-coat/Ag.

Fig. 6 shows the variation of the open circuit potential (OCP) as a function of time in the Ringer solution. The uncoated sample reached the pitting potential (-1.50 V) after approximately 5 hours of immersion (Fig.6, a). The initial OCP value for Mo-coat/Ag was -0.95 V (Fig. 6, curve b). Then, the OCP decreased until around -1.35 V , where it remained for approximately two days. A similar

response to that of the uncoated sample was obtained for Ce-coat/Ag (Fig. 6, curve c). In the case of Ce-Mo-coat/Ag, the OCP value is approximately -1.00 V after 72 h of immersion (Fig. 6, curve d). This potential value was still nobler than that of the bare electrode, indicating a superior anticorrosive performance of this coating.

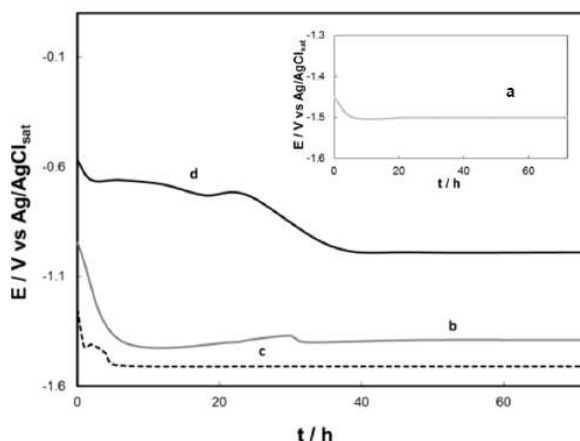


Figure 6. Time dependence of the OCP in the Ringer solution for: (a) bare AZ91D magnesium alloy, and the alloy covered with (b) Mo-coat/Ag, (c) Ce-coat/Ag and (d) Ce-Mo-coat/Ag.

To determine the concentration of ions released from the silver modified samples after 5 h of immersion in the Ringer solution, the electrolyte solutions were analyzed (Table 3). The results confirm that the Ce-Mo-coat/Ag *significantly decreased* the degradation velocity of the substrate.

Table 3. Concentration of magnesium species released in the Ringer solution after 5 h of immersion for the uncoated and coated AZ91D alloy.

Sample	Mg (mg/L)
AZ91D	3.90
Mo-coat/Ag	3.44
Ce-coat/Ag	2.73
Ce-Mo-coat/Ag	0.80

In order to confirm the anticorrosive performance of the silver-modified coatings, EIS measurements were also conducted in the Ringer solution. Fig. 7 shows the Nyquist diagrams for all modified coatings and the bare AZ91D Mg alloy (Fig. 7, curve a). Two capacitive loops and one inductive loop were observed for the bare electrode. It is known that the inductive loop is associated with the relaxation processes of adsorbed species such as $\text{Mg}(\text{OH})^+$ or $\text{Mg}(\text{OH})_2$ onto the electrode surface [37]. However, the response obtained for the silver-modified coatings does not present this behavior, indicating that there is no interaction between the metal surface and the corrosive solution. It has been reported in the literature that the bigger is the diameter of the semicircle the better is the corrosion resistance of the sample [38]. As it can be seen, the responses for the modified coatings present larger semicircles compared with that of the uncoated electrode, confirming that all the films improve the corrosion resistance of the alloy in the

Ringer solution. Among them, Ce-Mo-coat/Ag shows the best anticorrosive properties.

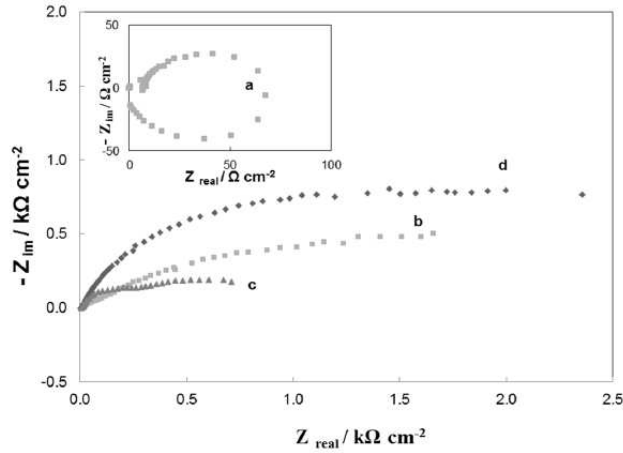


Figure 7. Nyquist plots of the impedance spectra at open circuit potential in the Ringer solution after 5 min of immersion for (a) bare AZ61D magnesium alloy, and the alloy covered with silver-modified coatings, (b) Mo-coat/Ag, (c) Ce-coat/Ag and (d) Ce-Mo-coat/Ag.

It is evident from the results presented above that Ce-Mo-coat/Ag provides the best protection to the substrate in simulated physiological conditions. In our previous work, it was demonstrated that the Ce-Mo-coat improves the corrosion resistance of AZ91D Mg alloys in a simulated physiological solution [26]. In order to know if the anticorrosive properties of Ce-Mo-coat are modified after Ag deposition, Tafel polarization curves were recorded. For comparison, the curves of Ce-Mo-coat, Ce-Mo-coat/Ag and that of the uncoated AZ91D alloy are presented (Fig. 8).

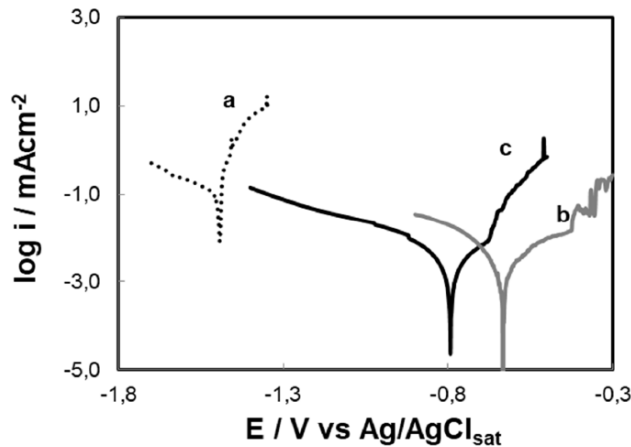


Figure 8. Tafel curves obtained in the Ringer solution for: (a) bare AZ91D magnesium alloy, and the alloy covered with: (b) Ce-Mo-coat and (c) Ce-Mo-coat/Ag.

Estimation of corrosion parameters (E_{corr} , cathodic (B_c) and anodic (B_a) Tafel slopes and corrosion current (i_{corr})) is shown in Table 4. The i_{corr} values obtained for the AZ91D magnesium alloy covered with the Ce-Mo-coat and the Ce-Mo-

coat/Ag are significantly lower than that of the bare AZ91D magnesium alloy. It can be noticed that the incorporation of silver species on the Ce-Mo-coat does not affect the anticorrosive performance of the unmodified film. By comparing the results obtained for both coatings, the Ce-Mo-coat/Ag and the unmodified film [26], a similar trend was observed in adherence force measurements, OCP tests, anodic polarization and analysis of the concentration of magnesium released in the Ringer solution. On the other hand, based on morphological characterization, it can be noticed that the incorporation of silver to the Ce-Mo-coat helps covering defects, such as pores and cracks [26].

Table 4. Corrosion parameters calculated from Tafel polarization plots for uncoated AZ91D, Mo-coat/Ag, Ce-coat/Ag and Ce-Mo-coat/Ag. The mean values and their standard deviation are presented.

	$E_{\text{corr}} / \text{V}$	$i_{\text{corr}} / \text{mAcm}^2$	B_a / V	B_c / V
AZ91D	-1.501 ± 0.050	0.1050 ± 0.0050	0.045	- 0.293
Ce-Mo-coat	$- 0.707 \pm 0.020$	0.002 ± 0.0005	0.176	- 0.123
Ce-Mo-coat/Ag	$- 0.796 \pm 0.030$	0.003 ± 0.0005	0.138	- 0.109

As it was stated, from the results obtained in this work, the most efficient corrosion protection of AZ91D Mg alloy is reached by the formation of the Ce-Mo-coat/Ag. It has been demonstrated that films composed by insoluble cerium oxides are able to protect Mg alloys [16, 39]. On the other hand, it is known that molybdenum acts as a corrosion inhibitor for Mg alloys. The formation of protective coatings containing molybdenum onto Mg alloys was reported [40-41]. In this sense, we suggest that the excellent corrosion resistance is associated with the presence of cerium and molybdenum species in the coating. In addition, we demonstrated that the anticorrosive performance of the Ce-Mo-coat was not affected by incorporation of silver to it. Thus, the film is able to provide simultaneously good corrosion resistance and antibacterial performance to the AZ91D Mg alloy surface.

Conclusions

Silver-modified coatings (Mo-coat/Ag, Ce-coat/Ag and Ce-Mo-coat/Ag) were obtained on the AZ91D magnesium alloy. Modified coatings have an antibacterial effect against ATCC 25922 *E. coli* Gram negative bacteria. The Ce-Mo-coat/Ag showed the best antibacterial behavior.

Comparing the anticorrosive performance of modified coatings, it could be seen that the Ce-Mo-coat/Ag film provides the best corrosion protection to AZ91D magnesium alloy in the Ringer solution. The presence of molybdenum and cerium species in the film increases the corrosion resistance which is associated with the inhibitory characteristics of these species. In spite of obtaining a denser structure by the addition of silver species, this modification does not affect the anticorrosive properties of Ce-Mo-coat, which are excellent. Thus, one can conclude that the Ce-Mo-coat/Ag is a promising material to impart *simultaneous corrosion resistance and antibacterial properties* to the AZ91D Mg alloy surface.

Acknowledgements

CONICET (PIP-112-201101-00055), ANPCYT (PICT-2015- 0726) and Universidad Nacional del Sur (PGI 24/M127), Bahía Blanca, Argentina are acknowledged for financial support.

References

1. Agarwal S, Curtin J, Duffy B et al. Biodegradable magnesium alloys for orthopaedic applications: A review on corrosion, biocompatibility and surface modifications. *Mater Sci Eng C*. 2016;68:948-963. 10.1016/j.msec.2016.06.020.
2. Chen Q, Thouas GA. Metallic implant biomaterials. *Mater Sci Eng R: Reports*. 2015;87:1–57. 10.1016/j.mser.2014.10.001.
3. Ballerini G, Bardi U, Bignucolo R et al. About some corrosion mechanisms of AZ91D magnesium alloy. *Corros Sci*. 2005;47(9):2173-2184. 10.1016/j.corsci.2004.09.018.
4. Hsiao HY, Tsung HC, Tsai WT. Anodization of AZ91D magnesium alloy in silicate-containing electrolytes. *Surf Coat Tech*. 2005;199(2-3):127-134. 10.1016/j.surfcoat.2004.12.010.
5. Pardo A, Merino MC, Coy AE et al. Pitting corrosion behavior of austenitic stainless steels combining effects of Mn and Mo additions. *Corros Sci*. 2008;50(6):1796-1806. 10.1016/j.corsci.2008.04.005.
6. Lemaitre C, Moneium A, Djoudjou R et al.. A statistical study of the role of molybdenum in the pitting resistance of stainless steels. *Corros Sci*. 1993;34(11):1913-1922. 10.1016/0010-938X(93)90027-E.
7. Mu S, Du J, Jiang H et al. Composition analysis and corrosion performance of a Mo-Ce conversion coating on AZ91 magnesium alloy. *Surf Coat Tech*. 2014;254:364-370. 10.1016/j.surfcoat.2014.06.044.
8. Hu J, Li Q, Zhong X, Zhang L et al. Composite anticorrosion coatings for AZ91D magnesium alloy with molybdate conversion coating and silicon sol-gel coatings. *Prog Org Coat*. 2009;66(3):199-205. 10.1016/j.porgcoat.2009.07.003.
9. Pezzato L, Brunelli K, Napolitani E et al. Surface properties of AZ91 magnesium alloy after PEO treatment using molybdate salts and low current densities. *Appl Surf Sci*. 2015;357(A):1031-1039. 10.1016/j.apsusc.2015.09.107.
10. Li X, Deng S, Fu H. Sodium molybdate as a corrosion inhibitor for aluminium in H₃PO₄ solution. *Corros Sci*. 2011;53(9):2748-2753. 10.1016/j.corsci.2011.05.002.
11. Kapp Jr. RW. Molybdenum. In: Michael Caplan, editor. Reference Module in Biomedical Sciences Encyclopedia of Toxicology. New Jersey: Monroe Township; 2014. p.383-388.

12. Forero Lopez AD, Lehr IL, Saidman SB. Anodisation of AZ91D magnesium alloy in molybdate solution for corrosion protection. *J Alloys Compd.* 2017;702:338-345. 10.1016/j.jallcom.2017.01.030.
13. Chen XB, Birbilis N, Abbott TB. Review of Corrosion-Resistant Conversion Coatings for Magnesium and Its Alloys. *Corrosion.* 2011;67(3):035005-1-035005-16. 10.5006/1.3563639.
14. Chen Y, Xu Z, Smith C et al. Recent advances on the development of magnesium alloys for biodegradable implants. *Acta Biomater.* 2014;10(11):4561-4573. 10.1016/j.actbio.2014.07.005.
15. Yasakau KA, Zheludkevich ML, Lamaka SV et al. Mechanism of corrosion inhibition of AA2024 by rare-earth compounds. *J Phys Chem B.* 2006;110:5515-5528. 10.1021/jp0560664.
16. Castano C, O'Keefe M, Fahrenholtz W. Cerium-based oxide coatings. *Curr Opin Solid State Mater Sci.* 2015;19:69-76. 10.1016/j.cossms.2014.11.005
17. Pommiers S, Fryret J, Castetbon A et al. Alternative conversion coatings to chromate for the protection of magnesium alloys. *Corros Sci.* 2014;84:135-146. 10.1016/j.corsci.2014.03.021.
18. Hornberger H, Virtanen S, Boccaccini AR. Biomedical coatings on magnesium alloys-A review. *Acta Biomater.* 2012;8(7):2442-2455. 10.1016/j.actbio.2012.04.012.
19. Cui X, Yang Y, Liu E et al.. Corrosion behaviors in physiological solution of cerium conversion coatings on AZ31 magnesium alloy. *Appl Surf Sci.* 2011;257(23): 9703-9709. 10.1016/j.apsusc.2011.04.141.
20. Montemor MF, Simoes AM, Ferreira MG et al. Composition and corrosion resistance of cerium conversion films. *Appl Surf Sci.* 2008;254(6):1806-1814. 10.1016/j.apsusc.2007.07.187.
21. Scholes MF, Soste C, Hughes AE et al. The role of hydrogen peroxide in the deposition of cerium-based conversion coatings. *Appl Surf Sci.* 2006;253:1770-1780. 10.1016/j.apsusc.2006.03.010.
22. Valdez B, Kiyota S, Stoytcheva M et al. Cerium-based conversion coatings to improve the corrosion resistance of aluminium alloy 6061-T6. *Corros Sci.* 2014;87:141-149. 10.1016/j.corsci.2014.06.023.
23. Eslamia M, Fedela M, Speranzab G et al. Study of selective deposition mechanism of cerium-based conversion coating on Rheo-HPDC aluminium-silicon alloys. *Electrochim Acta.* 2017;255:449-462. 10.1016/j.electacta.2017.09.182.
24. Sun J, Wang G. Preparation and corrosion resistance of cerium conversion coating on AZ91D magnesium alloy by a cathodic electrochemical treatment. *Surf Coat Tech.* 2014;254:42-48. 10.1016/j.surfcoat.2014.05.054.
25. Loperena AP, Lehr IL, Saidman SB. Formation of a cerium conversion coating on magnesium alloy using ascorbic acid as additive. Characterisation and anticorrosive properties of the formed films. *J Magnes Alloys.* 2016;4(4):278-285. 10.1016/j.jma.2016.10.002.
26. Lehr IL, Saidman SB. Corrosion protection of AZ91D magnesium alloy by a cerium molybdenum coating. The effect of citric acid as an additive. *J Magnes Alloys.* 2018;6(4):356-365. 10.1016/j.jma.2018.10.002.

27. Morones JR, Elechiguerra JL, Camacho A et al. The bactericidal effect of silver nanoparticles. *Nanotechnology*. 2005;16(10):2346-2353. 10.1088/0957-4484/16/10/059.
28. Ciacotich N, Ud Din R, Sloth JJ et al. An electroplated copper–silver alloy as antibacterial coating on stainless steel. *Surf Coat Tech*. 2018;35:96-104. 10.1016/j.surfcoat.2018.04.007.
29. Khalilpour P, Lampe K, Wagener M et al. Ag/SiO_xCy plasma polymer coating for antimicrobial protection of fracture fixation devices. *J Biomed Mater Res Part B: Appl Biomater*. 2010;94B(1):196-202. 10.1002/jbm.b.3164.
30. Bakhsheshi-rad HR, Hamzah E, Ismail AF et al. Bioactivity, in-vitro corrosion behavior, and antibacterial activity of silver–zeolites doped hydroxyapatite coating on magnesium alloy. *Trans Nanoferrous Metals Soc China*. 2018;28(8):1553-1562. 10.1016/S1003-6326(18)64797-1.
31. Kotoka R, Yamoah NK, Mensah-Darkwa K et al. Electrochemical corrosion behavior of silver doped tricalciumphosphate coatings on magnesium for biomedical application. *Surf Coat Tech*. 2016;292:99-109. 10.1016/j.surfcoat.2016.03.017.
32. Liu Z, Schade R, Luthringer B et al. Influence of the Microstructure and Silver Content on Degradation, Cytocompatibility, and Antibacterial Properties of Magnesium-Silver Alloys In Vitro. *Oxid Med Cell Longev*. 2017; 091265. 10.1155/2017/8091265
33. Clinical Laboratory Standards Institute. Performance standards for antimicrobial disk susceptibility tests; Approved standard-9th ed. CLSI document M2-A9. 26:1. Wayne, PA: Clinical Laboratory Standards Institute; 2006.
34. Bernard CH, Fan WY. Preparation of Ag stellar dendrites: modeling the growth of stellar snowflakes. *Crystal Growth and Desing*. 2014;14(11): 6067–6072. 10.1021/cg5012204.
35. Zhou Q, Wang S, Jia N et al. Synthesis of highly crystalline silver dendrites microscale nanostructures by electrodeposition. *Mater Lett*. 2006;60(29-30): 3789–3792. 10.1016/j.matlet.2006.03.115.
36. Nonaka T, Uemura Y, Enishi K et al. Antibacterial activity of resin-containing triethylenetetramine side chains and/or thiol groups–metal complexes. *J Appl Polym Sci*. 1996;62(10): 1651-1659. 10.1002/(SICI)1097-4628(19961205)62:10<1651::AID-APP17>3.0.CO;2-4.
37. Anik M, Celikten G. Analysis of the electrochemical reaction behavior of alloy AZ91 by EIS technique in H₃PO₄/KOH buffered K₂SO₄ solutions. *Corros Sci*. 2017;49(4):1878-1894. 10.1016/j.corsci.2006.10.016.
38. Mhaede M, Pastorek F, Hadzima B. Influence of shot peening on corrosion properties of biocompatible magnesium alloy AZ31 coated by dicalcium phosphate dihydrate (DCPD). *Mater Sci Eng: C*. 2014;C39:330-335. 10.1016/j.msec.2014.03.023.
39. Martínez L, Román E, de Segovia JL et al. Surface study of cerium oxide based coatings obtained by cathodic electrodeposition on zinc. *Appl Surf Sci*. 2011;257: 6202-6207. 10.1016/j.apsusc.2011.02.033.

40. Ishizaki T, Masuda Y, Teshima K. Composite film formed on magnesium alloy AZ31 by chemical conversion from molybdate/phosphate/fluorinate aqueous solution toward corrosion protection. *Surf Coat Technol.* 2013;217:76-83. 10.1016/j.surfcoat.2012.11.076.
41. Taylor SR, Chambers BD. Identification and characterization of nonchromate corrosion inhibitor synergies using high-throughput methods. *Corrosion.* 2008;64(3):255-270. 10.5006/1.3278470.